Acta Crystallographica Section D
Biological Crystallography
ISSN 0907-4449

L-Isoaspartate 115 of porcine β-trypsin promotes crystallization of its complex with bdellastasin

Ulrich Rester,[a]* Matthias Moser,[b] Robert Huber[a] and Wolfram Bode[a]

[a]Max-Planck-Institut für Biochemie, Abteilung Strukturforschung, Am Klopferspitz 18a, 82152 Martinsried, Germany, and [b]Ludwig-Maximilians-Universität München, Abteilung für Klinische Chemie und Klinische Biochemie, Klinikum der Universität – Innenstadt, Nußbaumstraße 20, 80336 München, Germany

Correspondence e-mail: rester@biochem.mpg.de

Received 29 September 1999
Accepted 23 February 2000

PDB Reference: β-trypsin–bdellastasin complex, 1eja.

Bdellastasin is a 59-amino-acid, cysteine-rich, antistasin-type inhibitor of sperm acrosin, plasmin and trypsin, isolated from the medicinal leech *Hirudo medicinalis*. The complex formed between bdellastasin and porcine β-trypsin has previously been crystallized in the presence of PEG in a tetragonal crystal form of space group $P4_32_12$ and has now been found to crystallize under high-salt conditions in the enantiomorphic space group $P4_12_12$. These structures have been solved and refined to 2.8 and 2.7 Å resolution, respectively. Bdellastasin turns out to have an antistasin-like fold exhibiting a bis-domainal structure. In the second new crystal form, the flexible N-terminal subdomain is rotated with respect to the C-terminal subdomain by about 90°, fitting into a cavity formed by symmetry-related trypsin molecules. The canonical inhibitor–proteinase interaction is restricted to the primary binding loop comprising residues Leu31–Lys36 of bdellastasin. During the refinement, a bound sodium ion occupying the calcium-binding site of the porcine β-trypsin component was discovered. This sodium ion is coordinated in a tetragonal–pyramidal manner, with the geometry of the enclosing loop slightly changed compared with the loop in the presence of calcium. In the crystal form of space group $P4_32_12$, the electron density for residue 115 of porcine β-trypsin clearly indicates the presence of a β-isomerized L-aspartic acid, which is placed in spatial proximity to segment Thr144–Gly148 of a symmetry-related trypsin molecule. This is the first structurally observed example of an L-isoaspartate in β-trypsin originating from Asn. A comparison with other known crystal structures of porcine β-trypsin–macromolecular inhibitor complexes suggests that the deamidation, isomerization and racemization of Asn115 is the key step in crystallization.

1. Introduction

Deamidation and racemization of L-asparagine and L-glutamine residues appear to be one of the most common non-enzymatic modifications of peptides and proteins (Clarke *et al.*, 1992; Gracy, 1992; Harding *et al.*, 1989; Wright, 1991). Studies on proteins and model peptides (Geiger & Clarke, 1987; Patel & Borchardt, 1990) have shown that under neutral or basic conditions the reaction proceeds *via* a succinimide derivative, which by spontaneous hydrolysis generates either an α-linked or a β-linked Asp (isoaspartyl) residue (Fig. 1). The rate of deamidation strongly depends on the nature of the side chain of the carboxyl-sided residue, with Asn–Gly or Asn–Ser being the most susceptible amino-acid pairs (Geiger & Clarke, 1987; Capasso *et al.*, 1989; Tyler-Cross & Schirch, 1991). The approximate ratio of α- to β-linked product is 1:3 for synthetic oligopeptides (Meinwald *et al.*, 1986) and for

proteins (Capasso *et al.*, 1991, 1996; Brennan & Clarke, 1993; Di Donato *et al.*, 1993).

In vivo, similar post-translational modifications of proteins have been reported for αA-crystallin (Fujii, Satoh *et al.*, 1994; Takemoto & Boyle, 1998) and αB-crystallin (Fujii, Ishibashi *et al.*, 1994) from young and aged human eye lenses, for β-amyloid peptide from Alzheimer's diseased brains (Roher *et al.*, 1993), for the microtubule-binding domain of tau (Watanabe *et al.*, 1999), for tubulin (Najbauer *et al.*, 1996) and for the high-mass methyl-accepting protein (HMAP) of the mammalian brain (David *et al.*, 1998).

Therefore, many organisms have evolved a strategy for reversing at least part of this damage by an enzymatic methylation reaction. The widely distributed cytosolic protein L-isoaspartate-(D-aspartate)-*O*-methyltransferase can initiate the conversion of L-isoaspartyl residues to L-aspartyl residues by forming the methyl ester (Brennan *et al.*, 1994) and thus starting the 'repair' pathway. Furthermore, an additional mechanism exists for the removal of isoaspartyl residues from polypeptides, including a catabolic pathway. The presence of such a degradative mechanism in *Escherichia coli* is supported by the existence of an isoaspartyl dipeptidase activity (Haley, 1968). It was shown that the enzyme catalyzes the hydrolysis of a specific subset of L-isoaspartyl-containing dipeptides but does not catalyze the cleavage of corresponding normal aspartyl dipeptides (Gary & Clarke, 1995).

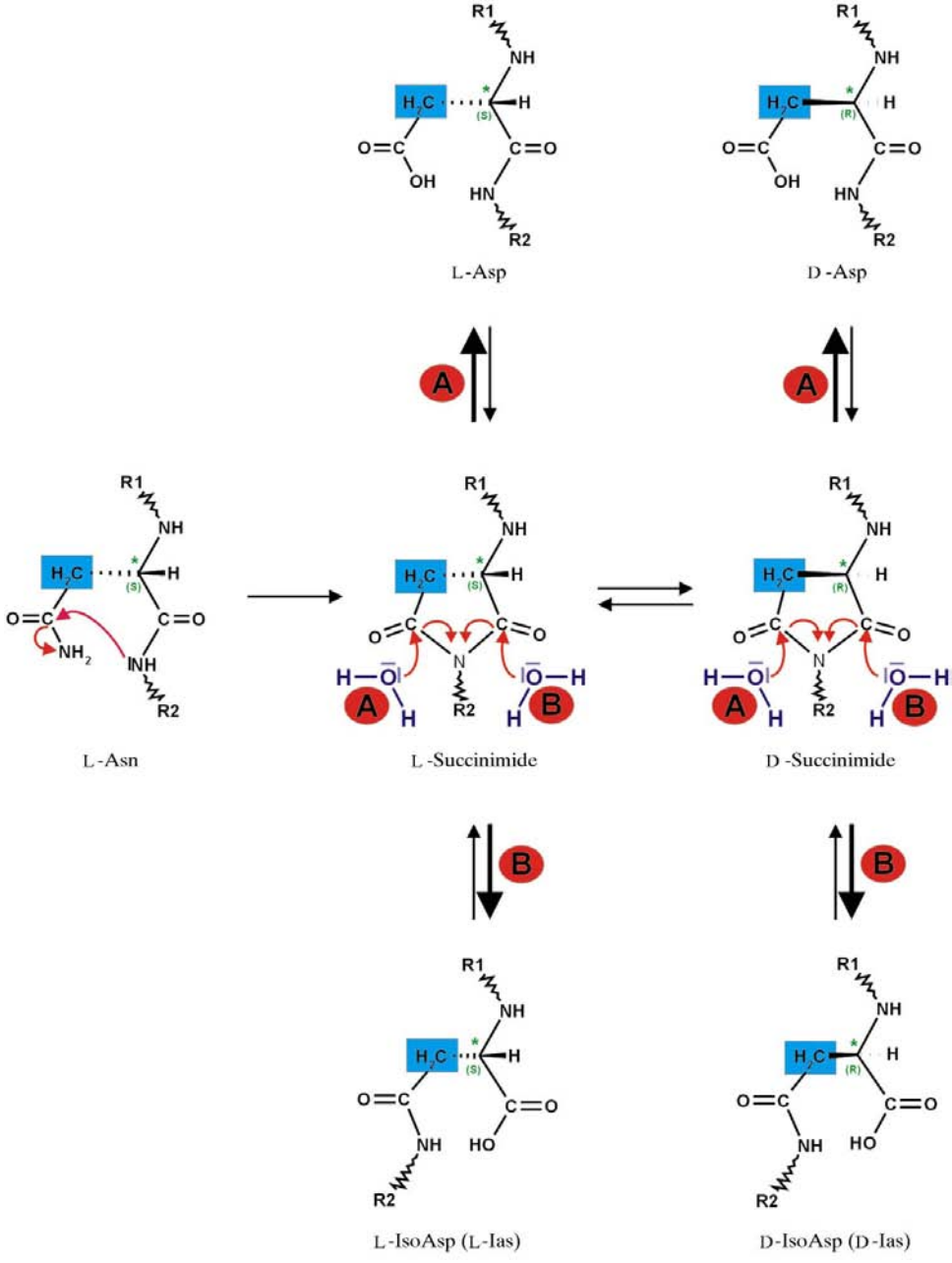

Figure 1
Pathways for the spontaneous deamidation, isomerization and racemization of asparaginyl and aspartyl residues. L-Asparaginyl (L-Asn) and L-aspartyl (L-Asp) residues can spontaneously convert *via* a succinimidyl intermediate to L-isoaspartate (L-Ias), D-aspartate (D-Asp) and D-isoaspartate (D-Ias) (scheme modified from Watanabe *et al.*, 1999).

Despite the numerous chemical and biological studies on deamidation, isomerization and racemization reactions in proteins, only a few crystallographic observations of β-linked Asp residues have so far been presented. This is not surprising, considering that labile Asn residues are normally located in flexible segments of the polypeptide chain characterized by a relatively poor electron density, which may well have prevented detection of alternative conformations. The first structural information regarding a deamidated protein comes from a neutron-diffraction study of aged bovine pancreatic trypsin (Kossiakoff, 1988), presenting a clear indication of three deamidated sites involving trypsin residues Asn48, Asn95 and Asn115. Previously, L-isoaspartate residues have been reported for Asn67 of bovine pancreatic ribonuclease A (Capasso *et al.*, 1996), for Asp45 of *Ustilago spherogena* ribonuclease U2 (Noguchi *et al.*, 1995) and recently for Asp101 of hen egg-white lysozyme (Noguchi *et al.*, 1998). Furthermore, a D-aspartate has been shown for residue Asn115 of porcine β-trypsin in complex with the leech-derived

Table 1
Data-processing statistics of BDA3.

Space group	$P4_12_12$
Unit-cell parameters (Å)	
a	70.02
b	70.02
c	119.48
V_m (Å^3 Da^{-1})	2.47 (50% H_2O)
Asymmetric unit content	1 complex
Limiting resolution (Å)	2.7
Number of crystals used	1
Number of significant measurements	51140
Number of independent reflections	8636
Completeness of data (%)	99.6 (99.6)†
Multiplicity overall (%)	5.9 (6.0)†
Average $R_{\rm merge}$‡	0.094 (0.353)†

† The values in parentheses correspond to the highest resolution shell, 2.85–2.70 Å. ‡ $R_{\rm merge} = \sum_{hkl}[(\sum_i|I_i - \langle I\rangle|)/\sum_i I_i]$ for equivalent observations.

Table 2
Final refinement statistics of BDA3.

Resolution (Å)	8.0–2.7
Reflections used for refinement (>2σ)	7986
Completeness (%)	96.6
R factor† (%)	19.1
$R_{\rm free}$‡ (%)	24.8
R.m.s. standard deviations	
Bond lengths (Å)	0.007
Bond angles (°)	1.546
Dihedral angles (°)	25.01
Improper angles (°)	0.777
R.m.s. *B*§ (Å^2)	1.752
Mean *B* factor, protein main chain (Å^2)	30.53
Mean *B* factor, protein side chain (Å^2)	31.95
Mean *B* factor, solvent (Å^2)	44.63
Total number of non-H protein atoms	2492
Number of active non-H protein atoms	2144
Number of water molecules	85
Metal atoms	1 Na^+
Φ, Ψ angle distribution¶	
Core region	155 (81.2)
Additionally allowed region	36 (18.8)
Generously allowed region	0 (0.0)
Disallowed region	0 (0.0)

† R factor = $\sum_{hkl}||F_{\rm obs}| - |F_{\rm calc}||/\sum_{hkl}|F_{\rm obs}|$. ‡ $R_{\rm free}$ is the cross-validation R factor computed for the test set of reflections (10% of total). § R.m.s. B is the r.m.s. deviation of the B factor of bonded atoms. ¶ As defined by *PROCHECK* (Laskowski *et al.*, 1993); the percentage distribution is given in parentheses.

tryptase inhibitor (LDTI; Di Marco & Priestle, 1997).

Here, we report the finding of an L-isoaspartate 115 detected in the porcine β-trypsin–bdellastasin complex structure. Bdellastasin is a 59 amino-acid, cysteine-rich, antistasin-type inhibitor directed toward sperm acrosin, plasmin and trypsin (Fritz *et al.*, 1971; Fritz & Krejci, 1976) and is found to tightly bind and inhibit trypsin as well as plasmin in the nanomolar range (K_i = 1.0 and 12 n*M*, respectively; Moser *et al.*, 1998). The inhibitor has recently been expressed in high yield in the yeast *Saccharomyces cerevisiae* (Moser *et al.*, 1998) and has been crystallized in complex with bovine and porcine β-trypsin in the monoclinic space group $P2_1$ and the tetragonal space group $P4_32_12$, respectively (Rester *et al.*, 1999). The structures have been solved and have been refined to 3.3 and 2.8 Å resolution, respectively. Bdellastasin displays an antistasin-like fold exhibiting a bis-domainal brick-shaped structure similar to that of the tissue kallikrein inhibitor hirustasin (Mittl *et al.*, 1997; Usón *et al.*, 1999). The interaction between bdellastasin and trypsin is restricted to the C-terminal subdomain of bdellastasin, particularly to its primary binding loop comprising residues Asp30–Glu38 (Rester *et al.*, 1999).

We have now obtained a second tetragonal crystal form of the porcine β-trypsin-bdellastasin complex under high-salt conditions. We have solved this structure in the enantiomorphic space group $P4_12_12$. The purpose of this paper is to communicate this structure and to analyze the role of crystallization conditions on the deamidation and isomerization of Asn115 of porcine β-trypsin and the effect of the β-isomerized L-aspartic acid 115 on the unit-cell formation.

2. Experimental

2.1. Crystallization

Recombinant bdellastasin was expressed in the yeast *S. cerevisiae* and purified as described previously (Moser *et al.*, 1998). Lyophilized porcine pancreatic trypsin type IX (E.C. 3.4.21.4) was purchased from Sigma. This β-trypsin was inhibited by a slight molar excess of bdellastasin in 100 m*M* sodium chloride, 50 m*M* MES, pH 6.5 for 1 h at 277 K, concentrated to 10 mg ml^{-1} by use of Microsep 3K tubes (Filtron) and dialyzed against 150 m*M* sodium chloride, 20 m*M* MES, pH 6.5. The bdellastasin–trypsin complex was crystallized by vapour diffusion using the 'sitting-drop' method (McPherson, 1989).

One crystal of the porcine β-trypsin–bdellastasin complex was obtained after 17 months in droplets containing 3 µl of protein solution and 1 µl of reservoir solution (4.0 *M* sodium formate, pH 7.7) equilibrated at 294 K against 1 ml of reservoir solution. This crystal was rod shaped and had maximal dimensions of 0.12 × 0.17 × 0.32 mm.

2.2. Data collection

Diffraction data were recorded at 293 K from one crystal of the porcine β-trypsin–bdellastasin complex with a 30 cm MAR Research imaging-plate detector system mounted on an RU-200 Rigaku rotating-anode X-ray generator operated at 5.4 kW (graphite-monochromated Cu $K\alpha$ radiation, λ = 1.54 Å). Images were processed using the *MOSFLM* package (Leslie, 1994) and data were scaled and merged with routines implemented in the *CCP*4 program suite (Collaborative Computational Project, Number 4, 1994). The data-processing statistics are summarized in Table 1.

2.3. Structure solution and refinement

The structure of the porcine β-trypsin–bdellastasin complex was solved by Patterson search techniques using the program *AMoRe* (Navaza, 1994). The orientation and position of the porcine β-trypsin–bdellastasin complex in the tetragonal crystal were determined using the structure of porcine pancreatic trypsin together with the bdellastasin fragment

28–57 (PDB accession code 1c9p; Rester *et al.*, 1999). The rotational search using data to 3.5 Å gave a single solution with a correlation value of 0.277, compared with 0.122 for the next highest peak. After applying the indicated rotation of $\alpha = -1.04$, $\beta = 64.54$, $\gamma = 347.9^\circ$, translation functions were calculated for the two enantiomorphic space groups $P4_12_12$ and $P4_32_12$. In $P4_32_12$, the highest peak was 1.05 times higher than the next one (correlation coefficient 0.333; R value 49.5%), while in $P4_12_12$ the translational search showed one solution with a correlation value of 0.639 over 0.391 for the next highest peak (R value 37.6%), identifying the latter space group as the correct one. After applying the suggested translation of $\Delta x = 0.2027$, $\Delta y = 0.3549$, $\Delta z = 0.2357$, rigid-body fitting with *AMoRe* brought the R value down to 33.4%, while the correlation coefficient increased to 0.722.

The structure of the porcine β-trypsin–bdellastasin complex was refined with *X-PLOR* (Brünger, 1992*a*,*b*) using the Engh & Huber (1991) parameters. R_{free} validation was based on a subset of 10% of reflections omitted during the entire refinement procedure. Starting with the properly rotated and translated model of porcine β-trypsin in complex with bdellastasin fragment 28–57, conventional Powell energy minimization and individual B-factor refinement against data in the resolution range 8.0–2.7 Å was carried out. In later stages of refinement, the maximum-likelihood algorithm implemented in the program *CNS* Development Version 0.3 (Brunger *et al.*, 1998) was used. Each round of refinement was followed alternately with manual model refitting using the program *O* (Jones *et al.*, 1991). The final refinement data are listed in Table 2.

3. Results and discussion

3.1. Quality of the final model

The structure of porcine β-trypsin complexed with bdellastasin has been refined to a crystallographic R value of 19.1 and an R_{free} of 24.8 at 2.7 Å resolution. Model building allowed the positioning of 221 trypsin residues, ten out of 59 bdellastasin residues, 85 water molecules and one sodium ion. Apart from a few surface-located side chains and the loop segment Ser146–Gly148, the trypsin moiety is almost completely defined in the electron-density map. On the other hand, the N-terminal and most of the C-terminal subdomain of the inhibitor, except for the primary binding loop from residues Leu31–Lys36 and parts of the secondary binding loop, lack any electron density, implying disorder relative to the trypsin moiety. A geometry check revealed that 81.2 and 18.8% of all non-glycine and non-proline residues lie within the most favoured and additionally allowed regions of the Ramachandran plot, respectively, as defined by *PROCHECK* (Laskowski *et al.*, 1993).

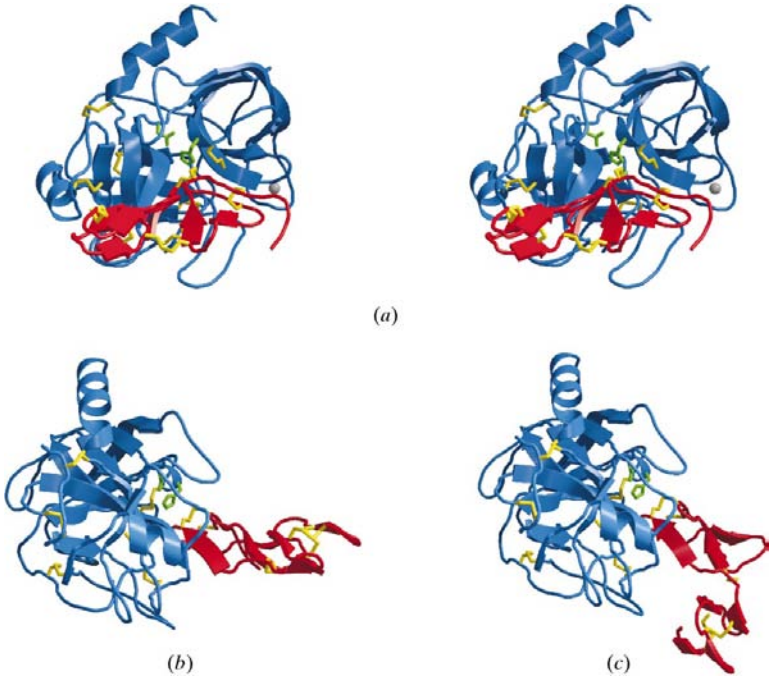

Figure 2
The antistasin-type inhibitor bdellastasin in complex with porcine β-trypsin. (*a*) Stereo ribbon diagram of the BDA2 complex formed between porcine β-trypsin (blue) and bdellastasin (red) in trypsin standard orientation, *i.e.* with the active-site cleft facing the viewer and a bound inhibitor chain running across the surface from left to right, and (*b*) rotated 90° around a vertical axis. Yellow connections indicate disulfide bridges and the calcium ion is shown as a grey ball. (*c*) The BDA3 complex formed between porcine β-trypsin (blue) and bdellastasin (red). Apart from the Leu31–Lys36 proteinase-binding loop of bdellastasin, which can be traced by electron density, the inhibitor is based on model building. These figures were produced with *BOBSCRIPT* (Esnouf, 1997) and *Raster3D* (Merritt & Murphy, 1994).

3.2. The porcine β-trypsin–bdellastasin complex structures

Previously, the antistasin-type cysteine-rich serine proteinase inhibitor bdellastasin had been crystallized in complex with bovine β-trypsin in the monoclinic space group $P2_1$ (BDA1) and in complex with porcine β-trypsin in the tetragonal space group $P4_32_12$ (BDA2; Rester *et al.*, 1999). Here, we describe the porcine β-trypsin–bdellastasin complex structure in a new crystal form belonging to the enantiomorphic space group $P4_12_12$ (BDA3). A comparison of the porcine β-trypsin molecules of the BDA2 and BDA3 complexes reveals an r.m.s. deviation of 0.38 Å for all 223 C^α positions, compared with 0.58 Å for 223 C^α atoms for the best defined bovine β-trypsin molecule (*D*) of the BDA1 complex.

In all BDA complexes, interactions between the inhibitor and the proteinase are restricted to the C-terminal subdomain of bdellastasin and particularly to the primary binding loop (residues 30–38). The reactive-site loop of bdellastasin in the BDA3 complex from Leu31 (P4) to Lys36 (P2′) is in direct contact with trypsin and binds to its active site in a substrate-like manner, *i.e.* with a main-chain conformation and intermolecular hydrogen-bond interactions similar to those seen in other canonically binding proteinase inhibitors (Bode & Huber, 1992). The relative orientation of the defined

bdellastasin segments in the BDA3 complex to trypsin is almost identical to the orientation observed in the BDA1 and BDA2 complexes, with virtually no differences in the main-chain conformation within the binding-loop region.

However, in the new crystal form the bdellastasin molecule cannot adopt the brick-shaped structure reported for the BDA1 and BDA2 complexes (Fig. 2*a,b*), *i.e.* with a stretched arrangement of the C-terminal and the N-terminal subdomain (Rester *et al.*, 1999). Owing to the tight crystal packing in the new crystal form, the flexible N-terminal subdomain of bdellastasin must be rotated by about 90° with respect to the N-terminal subdomain of the BDA1 complex (Fig. 2*c*) to fit into a cavity formed by symmetry-related trypsin molecules. This wedge-shaped structure is in agreement with the assumption that the N-terminal subdomain can rotate as a rigid body along the linker segment Ser29–Leu31 with respect to the C-terminal subdomain (Rester *et al.*, 1999).

3.3. A sodium ion occupying the calcium-binding site of porcine β-trypsin

During the refinement procedure, the presence of a bound sodium ion at the calcium-binding site of the porcine β-trypsin molecule in the tetragonal crystals of space group $P4_12_12$ (BDA3) became evident. Significant positive electron density at the $+6\sigma$ contouring level (Fig. 3*a*) clearly indicated the presence of a metal ion at the beginning of the refinement. However, a calcium ion entailed a negative electron density below -4σ after positional refinement (Fig. 3*a*) and a *B* value of 109.9 Å^2 after individual *B*-factor refinement. Therefore, the positive electron density was interpreted as a sodium ion according to the crystallization conditions and structural characteristics.

The sodium ion in the BDA3 structure has an occupancy of 1.0 and a *B* value of 36.3 Å^2 compared with an average *B* value of 31.9 Å^2 for its ligands. As can be seen in Fig. 3, the sodium ion is complexed by the carbonyl O atoms of Asn72 (2.3 Å, compared with 2.3 Å for the calcium ion in the BDA2 structure) and Val75 (2.4 Å, compared with 2.4 Å in BDA2) and by the side-chain O atoms Glu70 O$^{\varepsilon1}$ (2.5 Å, compared with 2.4 Å in BDA2) and Glu80 O$^{\varepsilon2}$ (2.4 Å, compared with 2.7 Å in BDA2) defining the central plane. The two axial ligands opposing each other in the octahedron are Glu77 and a more distant water molecule H_2O32 (4.7 Å, compared with 3.4 Å for H_2O69 in BDA2). Moreover, the Na^+ position is shifted out of the central plane by about 0.4 Å towards Glu77, allowing the Na^+ to make direct contacts with Glu77 O$^{\varepsilon1}$ (2.8 Å, compared with 4.5 Å in BDA2), *i.e.* different to the 'classical' water-mediated Ca^{2+} position in the BDA2 structure (Rester *et al.*, 1999). Furthermore, the side chain of Glu77 has moved by about 1.5 Å towards the sodium ion. This movement is reflected by larger shifts of up to 1.1 Å for the six C$^\alpha$ atoms of loop segment Asn72–Glu77, compared with an r.m.s. deviation of 0.38 Å for the 233 C$^\alpha$ atoms of the entire porcine β-trypsin molecules in the bdellastasin complexes of the enantiomorphic space groups $P4_12_12$ and $P4_32_12$. The sodium ion in the calcium-binding site of porcine β-trypsin displays some larger rearrangements compared with calcium and, owing to the close Glu77 and the distant water molecule H_2O32, exhibits a tetragonal pyramidal coordination, in contrast to tetragonal bipyramidal coordination (Bode & Schwager, 1975).

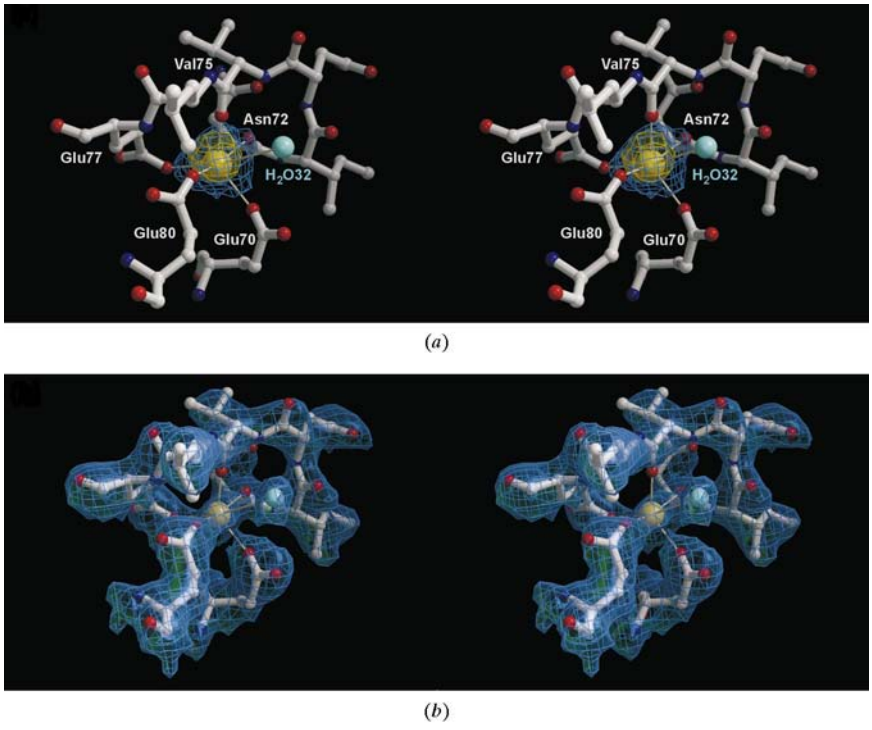

Figure 3
Stereoview of the trypsin calcium-binding loop in BDA3, with a sodium ion occupying the calcium-binding site. (*a*) The sodium ion (yellow ball) of porcine β-trypsin (white stick model) is shown together with $F_o - F_c$ difference density (-4σ, yellow; $+6\sigma$, blue). The displayed negative peak in the $F_o - F_c$ difference map is observed when a calcium ion is refined in this position. The water molecule H_2O32 is shown as a blue ball and possible electrostatic interactions of the sodium ion are indicated as white lines. (*b*) The final $2F_o - F_c$ electron density around the sodium ion contoured at 1.1σ. These figures were produced with *BOBSCRIPT* (Esnouf, 1997) and *Raster3D* (Merritt & Murphy, 1994).

3.4. L-Isoaspartate 115 of the porcine β-trypsin–bdellastasin complex

In the porcine β-trypsin–bdellastasin structure of the tetragonal space group $P4_12_12$ (BDA3), loop segment Leu114–Arg117 of the trypsin molecule can easily be traced in the $2F_o - F_c$ Fourier map (Fig. 4*a*). This loop segment is well defined and makes no direct crystal contacts to symmetry-related molecules. The electron density drawn at the 1σ contouring level clearly indicates the presence of the naturally occurring L-asparagine residue at position 115.

In contrast, in the porcine β-trypsin–bdellastasin complex of enantiomorphic space group $P4_32_12$ (BDA2; Rester *et al.*, 1999), residue 115 had been refined as L-isoaspartate (Ias115; Fig. 4*b*). The electron density, accounting for a short side chain and a quite long separation from the following α C atom, is neither in agreement with an L-Asn or L-Asp, nor with an D-Asn or D-Asp, but clearly indicates the presence of a β-isomerized L-aspartic acid for this trypsin residue. This L-isoaspartic acid presumably results from a spontaneous deamidation accompanied by simultaneous isomerization reactions *via* a five-membered succinimide ring. The $F_o - F_c$ difference map is relatively featureless for the L-isoaspartic acid and all crystallographic and stereochemical parameters are acceptable. Ias115 juxtaposes segment Thr144–Gly148 of a symmetry-related molecule (Fig. 4*b*), thereby making tight crystal contacts. The side-chain O atoms Ias115 $O^{\gamma1}$ and $O^{\gamma2}$ are within hydrogen-bonding distance (2.9 and 3.3 Å) of the hydrogen-bond donors Ser147 N and Ser146 N, respectively. Furthermore, Ias115 $O^{\gamma2}$ is linked to Thr144 O through the two hydrogen-bonded water molecules H_2O10 and H_2O43, Leu114 O interacts with Lys145 N^{ζ} (3.2 Å), and Ser116 O^{γ} is water-connected to Ser146 O^{γ}. These crystal contacts would also be possible for D-Asp (Fig. 4*c*), as observed in the porcine trypsin–LDTI complex (Di Marco & Priestle, 1997). Apart from the missing water-bridged Ser116 O^{γ}—Ser146 O^{γ} contact, the interaction pattern seems to be conserved, although the D-Asp115 $O^{\delta1}$—Ser147 N (2.6 Å) and D-Asp115 $O^{\delta2}$—Ser146 N (2.5 Å) interactions are slightly shorter (Table 3). It is thus tempting to speculate that the formation of this crystal form is associated with the deamidation and racemization of L-Asn115 to D-Asp115 and is particularly favoured for the isomerized product L-isoaspartate.

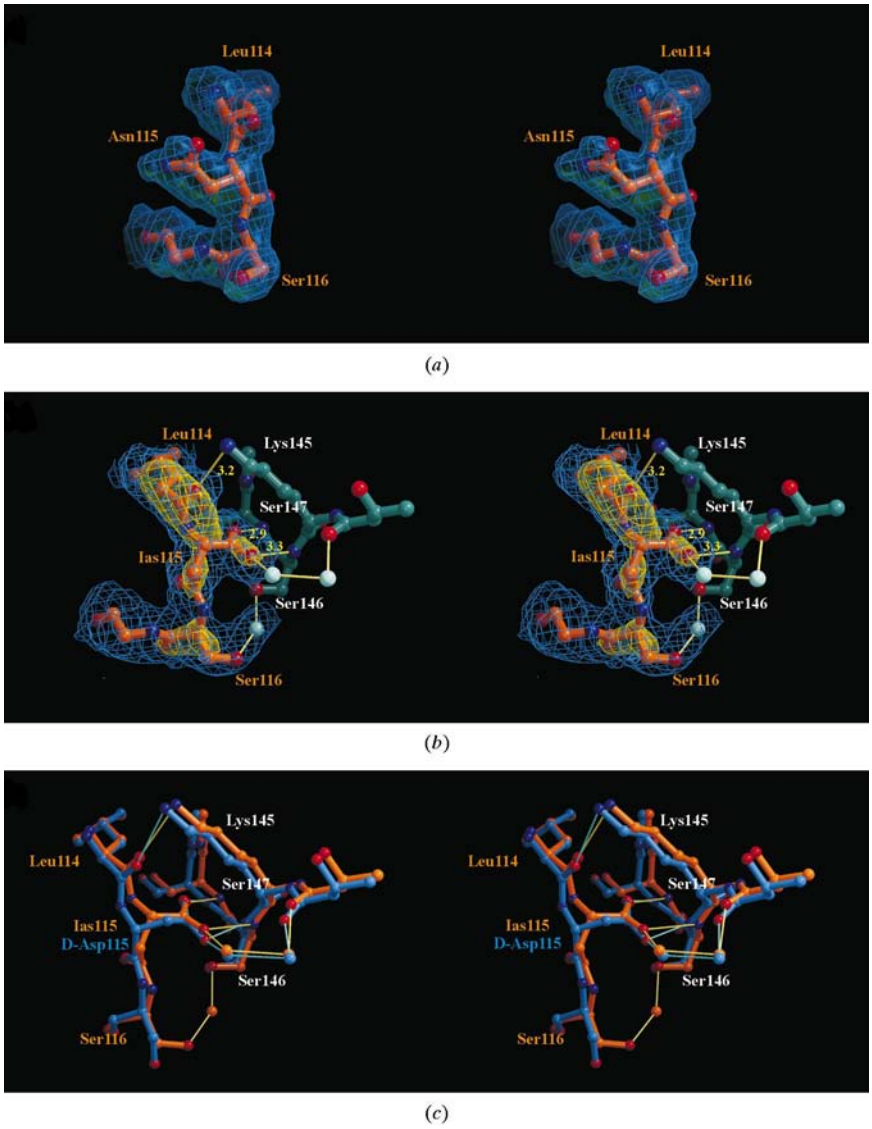

Figure 4
Stereoview of porcine trypsin around Asn115. (*a*) The loop segment Leu114–Arg117 of porcine β-trypsin in its bdellastasin complex of the tetragonal space group $P4_12_12$ (BDA3) is shown in orange. The final $2F_o - F_c$ electron-density map contoured at 1.0σ is shown in light blue. (*b*) The structure around Asn115 of the BDA2 complex, interpreted and refined as an L-isoaspartate (Ias115), is shown in orange, while part of a symmetry-related trypsin molecule making hydrogen bonds with Ias115 and with water molecules (blue balls) is shown in green. The $F_o - F_c$ difference map ($+3\sigma$, yellow) was calculated with coordinates from which residues 113–117 had been omitted. The final $2F_o - F_c$ electron-density map contoured at 1.2σ is shown in light blue. Hydrogen bonds are indiacted as yellow lines. (*c*) Stereo superposition of the structure around Ias115 (orange) with D-Asp115 (blue) and the corresponding loop segments 144–147 of the symmetry-related trypsin molecules. The structures are shown as ball-and-stick models, water molecules are shown as orange or blue balls and hydrogen bonds as yellow or blue lines, respectively. These figures were produced with *BOBSCRIPT* (Esnouf, 1997) and *Raster3D* (Merritt & Murphy, 1994).

3.5. Crystallization effects of the L-isoaspartate and D-aspartate formation

Three porcine β-trypsin molecules in complex with macromolecular inhibitors have previously been crystallized in the tetragonal space group $P4_32_12$. These are the two porcine β-trypsin–LDTI complex structures LDTI1 and LDTI2 [PDB accession codes 1an1 (Di Marco & Priestle, 1997) and 1ldt (Stubbs *et al.*, 1997), respectively] and the porcine β-trypsin–bdellastasin complex structure BDA2 (PDB accession code 1c9p; Rester *et al.*, 1999). For LDTI1, residue Asn115 has been refined as D-Asp115, for LDTI2 the interpretation of the electron density at residue 115 is consistent with D-Asp (M. Stubbs, personal communication) and for BDA2 the electron density clearly indicates the presence of a β-isomerized L-aspartic acid. Interestingly, the unit-cell parameters

Table 3
Comparison of intermolecular contacts of Ias115 (BDA2) and D-Asp115 (LDTI1) with the loop segment 144–147 of a symmetry-related trypsin molecule (SYM).

Trypsin (SYM)	Trypsin (BDA2)	Distance (Å) (BDA2)	Distance (Å) (LDTI1)	Trypsin (LDTI1)	Trypsin (SYM)
Lys145 N^{ζ}	Leu114 O	3.2	3.2	Leu114 O	Lys145 N^{ζ}
Ser146 N	Ias115 $O^{\gamma 2}$	3.3	2.5	D-Asp115 $O^{\delta 2}$	Ser146 N
Ser147 N	Ias115 $O^{\gamma 1}$	2.9	2.6	D-Asp115 $O^{\delta 1}$	Ser147 N
Thr144 O	H_2O10 O	2.9	3.5	H_2O64 O	Thr144 O
H_2O10 O	Ias115 $O^{\gamma 2}$	2.9	2.9	D-Asp115 $O^{\delta 2}$	H_2O64 O
Thr144 O	H_2O43 O	2.7	2.6	H_2O32 O	Thr144 O
H_2O43 O	H_2O10 O	2.8	3.4	H_2O64 O	H_2O32 O
Ser146 O^{γ}	H_2O130 O	2.3			
H_2O130 O	Ser116 O^{γ}	2.3			

Table 4
Deamidation, racemization and isomerization of Asn115 of porcine β-trypsin effect on unit cell formation.

	BDA3	BDA2	LDTI1	LDTI2
Crystallographic data				
PDB entry	1eja	1c9p	1an1	1ldt
Space group	$P4_12_12$	$P4_32_12$	$P4_32_12$	$P4_32_12$
Unit-cell parameters (Å)				
a	70.02	63.33	63.70	63.40
b	70.02	63.33	63.70	63.40
c	119.48	130.61	130.86	131.20
Crystallization				
Precipitant	4.0 *M* sodium formate	20%(*w*/*v*) PEG 4K, 20%(*v*/*v*) 2-propanol	30%(*v*/*v*) 2-propanol	10%(*w*/*v*) PEG 6K, 2.3 *M* phosphate
pH	7.7	7.5	8.5	8.0
Buffer	—	0.1 *M* HEPES	0.1 *M* Tris–HCl	—
Time (months)	17	18	27	—
Mutations	—	L-Ias115	D-Asp115	(D-Asp115)
Literature	This work	Rester *et al.* (1999)	Di Marco & Priestle (1997)	Stubbs *et al.* (1997)

are nearly identical for these three complexes and the crystallization parameters are similar (Table 4). The similarity of these complex structures is reflected by an r.m.s. deviation of 0.38 Å for 1784 C^{α} atoms for LDTI1 and of 0.36 Å for 1784 C^{α} positions for LDTI2, compared with the eight BDA2 trypsin molecules in the unit cell (Fig. 5). However, the presence of PEG or alcohol as precipitant seems to be necessary for crystallization in the tetragonal space group $P4_32_12$. This result is in agreement with the BDA3 complex crystallized from high-salt conditions in the enantiomorphic space group $P4_12_12$. In this crystal form, the electron density at residue 115 corresponds to the naturally occurring L-Asn and the loop segment Leu114–Ser116 forms no direct crystal contacts to symmetry-related trypsin molecules. Furthermore, as incubation times of 17 up to 27 months seem to be essential for the crystallization process in order to form the succinimidyl intermediates.

From this, we propose a model for the crystallization process of porcine β-trypsin in complex with macromolecular inhibitors in the tetragonal space group $P4_32_12$ which is similar to the model of the early stage of crystallization of lysozyme (Igarashi *et al.*, 1999): the driving force for crystallization seems to be the formation of hydrophobic interactions between the trypsin molecules. The succinimide formation in residue Asn115, connected with the disappearance of an $-NH_2$ group on the protein surface (Fig. 1), results in a lower solubility of the succinimide-115 trypsin, as observed for succinimide hen egg-white lysozyme (Miyawaki *et al.*, 1996). Consequently, by lowering the protein solubility, succinimide-115 trypsin seems to play a crucial role as a 'transition-state intermediate' in crystal nucleation and crystal growth.

Consequently, owing to the reorientation of the side chain in position 115 and the spatial orientation of the isomerization product Ias115 and the racemization product D-Asp115 (Fig. 4*c*), the loop segment Leu114–Ser116 is able to form favourable electrostatic interactions with segment Thr144–Gly148 of another β-trypsin molecule, thus tightly clamping the trypsin molecules together.

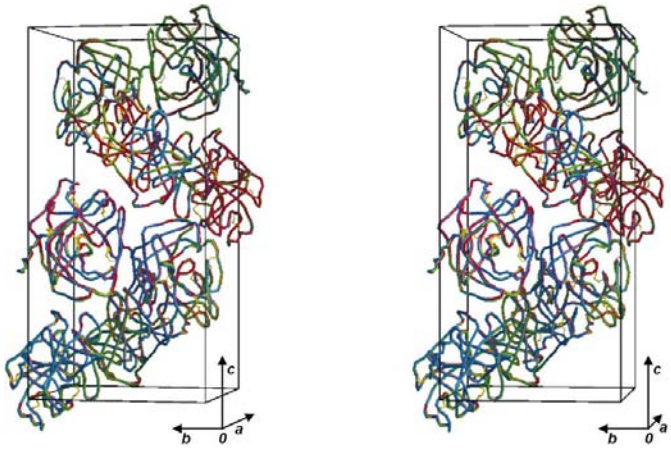

Figure 5
Stereo picture of the eight porcine β-trypsin molecules of the LDTI1, LDTI2 and BDA2 complex (coloured blue, green and red, respectively) superimposed in the unit cell of tetragonal space group $P4_32_12$. Yellow connections indicate disulfide bridges. The cell axes are displayed. This figure was produced with *BOBSCRIPT* (Esnouf, 1997) and *Raster3D* (Merritt & Murphy, 1994).

We thank E. Auerswald for fruitful discussions. This work was supported by the Sonderforschungsbereich 469 from the University of Munich.

References

Bode, W. & Huber, R. (1992). *Eur. J. Biochem.* **204**, 433–451.
Bode, W. & Schwager, P. (1975). *J. Mol. Biol.* **98**, 693–717.
Brennan, T. V., Anderson, J. W., Jia, Z., Waygood, E. B. & Clarke, S. (1994). *J. Biol. Chem.* **269**, 24586–24595.
Brennan, T. V. & Clarke, S. (1993). *Protein Sci.* **2**, 331–338.
Brünger, A. T. (1992*a*). *X-PLOR Version* 3.1. *A System for X-ray Crystallography and NMR.* New Haven, Connecticut, USA.
Brünger, A. T. (1992*b*). *Nature (London)*, **355**, 472–475.
Brunger, A. T., Adams, P. D., Clore, G. M., Delano, W. L., Gros, P., Grosse-Kunstleve, R. W., Jiang, J.-S., Kuszewski, J., Nilges, N., Pannu, N. S., Read, R. J., Rice, L. M., Simonson, T. & Warren, G. L. (1998). *Acta Cryst.* D**54**, 905–921.
Capasso, S., Di Donato, A., Esposito, L., Sica, F., Sorrentino, G., Vitagliano, L., Zagari, A. & Mazzarella, L. (1996). *J. Mol. Biol.* **257**, 492–496.
Capasso, S., Mazzarella, L., Sica, F. & Zagari, A. (1989). *Pept. Res.* **2**, 195–200.
Capasso, S., Mazzarella, L. & Zagari, A. (1991). *Pept. Res.* **4**, 234–238.
Collaborative Computational Project, Number 4 (1994). *Acta Cryst.* D**50**, 760–763.
Clarke, S., Stephenson, R. C. & Lowenson, D. (1992). *Stability of Protein Pharmaceuticals, Part A: Chemical and Physical Pathways of Protein Degradation*, edited by T. J. Ahern & M. C. Manning, pp. 1–29. New York: Plenum Press.
David, C. L., Orpiszewski, J., Zhu, X. C., Reissner, K. J. & Aswad, D. W. (1998). *J. Biol. Chem.* **273**, 32063–32070.
Di Donato, A., Ciardiello, M. A., de Nigris, M., Piccoli, R., Mazzarella, L. & D'Alessio, G. (1993). *J. Biol. Chem.* **268**, 4745–4751.
Di Marco, S. & Priestle, J. P. (1997). *Structure* **5**, 1465–1474.
Engh, R. A. & Huber, R. (1991). *Acta Cryst.* A**47**, 392–400.
Esnouf, R. M. (1997). *J. Mol. Graph.* **15**, 132–134.
Fritz, H., Gebhardt, M., Meister, R. & Fink, E. (1971). *Proceedings of the International Research Conference on Proteinase Inhibitors*, edited by H. Fritz & H. Tschesche, pp. 271–280. Berlin: Walter de Gruyter.
Fritz, H. & Krejci, K. (1976). *Methods Enzymol.* **45**, 797–806.
Fujii, N., Ishibashi, Y., Satoh, K., Fujino, M. & Harada, K. (1994). *Biochim. Biophys. Acta*, **1204**, 157–163.
Fujii, N., Satoh, K., Harada, K. & Ishibashi, Y. (1994). *J. Biochem.* **116**, 663–669.
Gary, J. D. & Clarke, S. (1995). *J. Biol. Chem.* **270**, 4076–4087.
Geiger, T. & Clarke, S. (1987). *J. Biol. Chem.* **262**, 785–794.
Gracy, R. W. (1992). *Stability of Protein Pharmaceuticals, Part A: Chemical and Physical Pathways of Protein Degradation*, edited by T. J. Ahern & M. C. Manning, pp. 119–145. New York: Plenum Press.
Haley, E. E. (1968). *J. Biol. Chem.* **243**, 5748–5752.
Harding, J. J., Beswick, H. T., Ajiboye, R., Huby, R., Blakytny, R. & Rixon, K. C. (1989). *Mech. Ageing Dev.* **50**, 7–16.
Igarashi, K., Azuma, M., Kato, J. & Ooshima, H. (1999). *J. Crystal Growth*, **204**, 191–200.
Jones, T. A., Zou, J.-Y., Cowan, S. W. & Kjeldgaard, M. (1991). *Acta Cryst.* A**47**, 110–119.
Kossiakoff, A. A. (1988). *Science*, **240**, 191–194.
Laskowski, R. A., MacArthur, M. W., Moss, S. D. & Thornton, J. M. (1993). *J. Appl. Cryst.* **26**, 283–291.
Leslie, A. G. W. (1994). *MOSFLM User Guide, MOSFLM Version* 5.20. MRC Laboratory of Molecular Biology, Cambridge, UK.
McPherson, A. (1989). *Preparation and Analysis of Protein Crystals.* Malabar: Krieger Publishing Co.
Meinwald, Y. C., Stimson, E. R. & Scheraga, H. A. (1986). *Int. J. Pept. Protein Res.* **28**, 79–84.
Merritt, E. A. & Murphy, M. E. P. (1994). *Acta Cryst.* D**50**, 869–873.
Mittl, P. R., Di Marco, S., Fendrich, G., Pohlig, G., Heim, J., Sommerhoff, C., Fritz, H., Priestle, J. P. & Grütter, M. G. (1997). *Structure*, **5**, 253–264.
Miyawaki, K., Noguchi, S., Harada, S. & Satow, Y. (1996). *J. Crystal Growth*, **168**, 292–296.
Moser, M., Auerswald, E., Mentele, R., Eckerskorn, C., Fritz, H. & Fink, E. (1998). *Eur. J. Biochem.* **253**, 212–220.
Najbauer, J., Orpiszewski, J. & Aswad, D. W. (1996). *Biochemistry*, **35**, 5183–5190.
Navaza, J. (1994). *Acta Cryst.* A**50**, 157–163.
Noguchi, S., Miyawaki, K. & Satow, Y. (1998). *J. Mol. Biol.* **278**, 231–238.
Noguchi, S., Satow, Y., Uchida, T., Sasaki, C. & Matsuzaki, T. (1995). *Biochemistry*, **34**, 15583–15591.
Patel, K. & Borchardt, R. T. (1990). *Pharm. Res.* **7**, 703–711.
Rester, U., Bode, W., Moser, M., Parry, M. A. A., Huber, R. & Auerswald, E. (1999). *J. Mol. Biol.* **293**, 93–106.
Roher, A. E., Lowenson, J. D., Clarke, S., Wolkow, C., Wang, R., Cotter, R. J., Reardon, I. M., Zurcher-Neely, H. A., Heinrikson, R. L. & Ball, M. J. (1993). *J. Biol. Chem.* **268**, 3072–3083.
Stubbs, M. T., Morenweiser, R., Sturzebecher, J., Bauer, M., Bode, W., Huber, R., Piechottka, G. P., Matschiner, G., Sommerhoff, C. P., Fritz, H. & Auerswald, E. A. (1997). *J. Biol. Chem.* **272**, 19931–19937.
Takemoto, L. & Boyle, D. (1998). *Biochemistry*, **37**, 13681–13685.
Tyler-Cross, R. & Schirch, V. (1991). *J. Biol. Chem.* **266**, 22549–22556.
Usón, I., Sheldrick, G. M., La Fortelle, E., Bricogne, G., Di Marco, S., Priestle, J. P., Grütter, M. G. & Mittl, P. R. E. (1999). *Structure*, **7**, 55–63.
Watanabe, A., Takio, K. & Ihara, Y. (1999). *J. Biol. Chem.* **274**, 7368–7378.
Wright, H. T. (1991). *Crit. Rev. Biochem. Mol. Biol.* **26**, 1–52.